The oceanic sink for anthropogenic CO_2

Christopher L. Sabine[1]*, Richard A. Feely[1], Nicolas Gruber[2], Robert M. Key[3], Kitack Lee[4], John L. Bullister[1], Rik Wanninkhof[5], C.S. Wong[6], Douglas W.R. Wallace[7], Bronte Tilbrook[8], Frank J. Millero[9], Tsung-Hung Peng[5], Alexander Kozyr[10], Tsueno Ono[11], and Aida F. Rios[12]

Using inorganic carbon measurements from an international survey effort in the 1990s and a tracer based separation technique, we estimate a global oceanic anthropogenic CO_2 sink for the period from 1800 to 1994 of 118±19 Pg C. The oceanic sink accounts for ~48% of the total fossil fuel and cement manufacturing emissions, implying that the terrestrial biosphere was a net source of CO_2 to the atmosphere of about 39±28 Pg C for this period. The current fraction of total anthropogenic CO_2 emissions stored in the ocean appears to be about one third of the long term potential.

[1] NOAA Pacific Marine Environmental Laboratory, 7600 Sand Point Way NE, Seattle, WA 98115, USA.
[2] University of California Los Angeles, IGPP & Department of Atmospheric and Oceanic Sciences, , Los Angeles, CA 90095, USA
[3] Princeton University, AOS Program, Forrestal Campus/Sayre Hall, Princeton, NJ 08533, USA
[4] Pohang University of Science and Technology, San 31, Nam-gu, Hyoja-dong, Pohang 790-784, South Korea
[5] NOAA Atlantic Oceanographic and Meteorological Laboratory, 4301 Rickenbacker Cswy., Miami, FL 33149, USA
[6] Institute of Ocean Sciences, Climate Chemistry Laboratory, PO Box 6000, Sidney, B.C. V8L 4B2, Canada
[7] Universitat Kiel, Institut fuer Meereskunde, Duesternbrooker Weg 20, D-24105 Kiel, Germany
[8] CSIRO Marine Research and Antarctic Climate and Ecosystem Cooperative Research Center, Hobart Tasmania 7001, Australia
[9] University of Miami, RSMAS-Div. of Marine and Atm. Sciences, 4600 Rickenbacker Causeway, Miami, FL 33149, USA
[10] CDIAC, Oak Ridge National Laboratory, U.S. Department of Energy, Mail Stop 6335, Oak Ridge, TN 37831-6335, USA
[11] FRSGC/IGCR, Sumitomo Hamamatsu-cho, bldg. 4F, 1-18-16 Hamamatsutyo, Minato-ku, 105-0013, Japan
[12] Instituto de Investigaciones Marinas.CSIC, c/Eduardo Cabello, 6, 36208 Vigo, Spain
* To whom correspondence should be addressed. E-mail: chris.sabine@noaa.gov

Since the beginning of the industrial period in the late 18th century, i.e. over the anthropocene (*1*), mankind has emitted large quantities of CO_2 into the atmosphere, mainly as a result of fossil fuel burning, but also because of land-use practices, e.g. deforestation (*2)*. Measurements and reconstructions of the atmospheric CO_2 history reveal, however, that less than half of these emissions remain in the atmosphere (*3*). The anthropogenic CO_2 that did not accumulate in the atmosphere must have been taken up by the ocean, by the land biosphere, or by a combination of both. The relative roles of the ocean and land biosphere as sinks for anthropogenic CO_2 over the anthropocene are currently not known. Although the anthropogenic CO_2 budget for the last two decades, i.e. the 1980s and 1990s, has been investigated in detail (*3*), the estimates of the ocean sink have not been based on direct measurements of changes in the oceanic inventory of dissolved inorganic carbon (DIC).

Recognizing the need to constrain the oceanic uptake, transport, and storage of anthropogenic CO_2 for the anthropocene and to provide a baseline for future estimates of oceanic CO_2 uptake, two international ocean research programs, the World Ocean Circulation Experiment (WOCE) and the Joint Global Ocean Flux Study (JGOFS), jointly conducted a comprehensive survey of inorganic carbon distributions in the global ocean in the 1990s (*4*). After completion of the US field program in 1998, a five year effort was begun to compile and rigorously quality control the US and international data sets including a few pre-WOCE data sets in regions that were data limited (*5*). The final data set consists of 9618 hydrographic stations collected on 95 cruises, which represents the most accurate and comprehensive view of the global ocean inorganic carbon

distribution available (*6*). As individual basins were completed, the ocean tracer based ΔC* method (*7*) was used to separate the anthropogenic CO_2 component from the measured DIC concentrations (*8-10*). Here we synthesize the individual ocean estimates to provide an ocean data-constrained global estimate of the cumulative oceanic sink for anthropogenic CO_2 for the period from ~1800 to 1994 (*11*).

Distribution and Inventories of Anthropogenic CO_2 in the Ocean

The objectively gridded individual sample estimates were vertically integrated to produce the column inventory map shown in Fig. 1. Since the global survey had limited data coverage in the marginal basins and the Arctic Ocean (north of 65°N), these areas were excluded from the mapped regions. The cumulative oceanic anthropogenic CO_2 sink in 1994, for the ocean region shown in Fig. 1, is 106±17 Pg C. Accounting for the excluded regions we estimate a global anthropogenic CO_2 sink of 118±19 Pg C. The uncertainty in the total inventory is based on uncertainties in the anthropogenic CO_2 estimates and mapping errors (*11*).

Figure 1 shows that this anthropogenic CO_2 is not evenly distributed throughout the oceans. The highest vertically integrated concentrations are found in the North Atlantic, leading this ocean basin to store 23% of the global oceanic anthropogenic CO_2, despite covering only 15% of the global ocean area (see Table S1). By contrast, the Southern Ocean south of 50ºS has very low vertically integrated anthropogenic CO_2 concentrations, containing only 9% of the global inventory. Over 40% of the global inventory is found in the region between 50ºS and 14ºS because of the substantially higher vertically integrated concentrations and the large ocean area in these latitude bands

(Fig. 1, Table S1). Approximately 60% of the total oceanic anthropogenic CO_2 inventory is stored in the Southern Hemisphere oceans, roughly in proportion to the larger ocean area of this hemisphere.

Figure 2 shows the anthropogenic CO_2 distributions along representative meridional sections in the Atlantic, Pacific and Indian oceans for the mid 1990s. Because anthropogenic CO_2 invades the ocean by gas exchange across the air-sea interface, the highest concentrations of anthropogenic CO_2 are found in near-surface waters. Away from deep water formation regions, the time scales for mixing of near-surface waters downward into the deep ocean can be centuries, and as of the mid-1990's the anthropogenic CO_2 concentration in most of the deep ocean remained below the detection limit for the ΔC^* technique.

Variations in surface concentrations are related to the length of time that the waters have been exposed to the atmosphere and to the buffer capacity, or Revelle Factor for seawater (*12, 13*). This factor describes how the partial pressure of CO_2 in seawater (pCO_2) changes for a given change in DIC. Its value is proportional to the ratio between DIC and alkalinity, where the latter term describes the oceanic charge balance. Low Revelle Factors are generally found in the warm tropical and subtropical waters and high Revelle Factors are found in the cold high latitude waters (Fig. 3). The capacity for ocean waters to take up anthropogenic CO_2 from the atmosphere is inversely proportional to the value of the Revelle Factor, hence the lower the Revelle Factor, the higher the oceanic equilibrium concentration of anthropogenic CO_2 for a given atmospheric CO_2 perturbation. The highest anthropogenic CO_2 concentrations (~60 μmol kg^{-1}) are found in

the subtropical Atlantic surface waters because of the low Revelle Factors in that region. By contrast, the near-surface waters of the North Pacific have a higher Revelle Factor at comparable latitudes and consequently lower anthropogenic CO_2 concentrations primarily because North Pacific alkalinity values are as much as 100 μmol kg^{-1} lower than those in the North Atlantic (Fig. 3).

Approximately 30% of the anthropogenic CO_2 is found shallower than 200 m and nearly 50% above 400 m depth. The global average depth of the 5 μmol kg^{-1} contour is approximately 1000 m. The majority of the anthropogenic CO_2 in the ocean is, therefore, confined to the thermocline, i.e. the region of the upper ocean, where temperature changes rapidly with depth. Variations in the penetration depth of anthropogenic CO_2 are determined by how rapidly the anthropogenic CO_2 that has accumulated in the near surface waters is transported into the ocean interior. This transport occurs primarily along surfaces of constant density called isopycnal surfaces.

The deepest penetrations are associated with convergence zones at temperate latitudes where water that has recently been in contact with the atmosphere can be transported into the ocean interior. The isopycnal surfaces in these regions tend to be thick and inclined providing a pathway for the movement of anthropogenic CO_2 laden waters into the ocean interior. Low vertical penetration is generally observed in regions of upwelling, such as the Equatorial Pacific, where intermediate depth waters, low in anthropogenic CO_2, are transported toward the surface. The isopycnal layers in the tropical thermocline tend to be shallow and thin minimizing the movement of anthropogenic CO_2 laden waters into the ocean interior.

Figure 4a shows the distribution of anthropogenic CO_2 on a relatively shallow isopycnal surface (see depths in Fig. 2) with a potential density (σ_θ) of 26.0. Approximately 20% of the anthropogenic CO_2 is stored in waters with potential densities equal to or less than this surface. The highest concentrations are generally found closest to where this density intersects the surface, referred to as the outcrop. Concentrations decrease away from these outcrops in the Indian and Pacific oceans primarily reflecting the aging of these waters, i.e. these waters were exposed to lower atmospheric CO_2 concentrations when they were last in contact with the atmosphere. The Atlantic waters do not show this trend because the 26.0 σ_θ surface is much shallower and therefore relatively well connected to the ventilated surface waters throughout most of the Atlantic (Fig. 2a, 4a).

The formation and transport of mode and intermediate waters is the primary mechanism for moving anthropogenic CO_2 to intermediate depths. The spatial distribution of anthropogenic CO_2 in these intermediate waters is illustrated with the 27.3 σ_θ surface (Fig. 4b), whose mean depth is about 900 m. As with the 26.0 σ_θ surface, anthropogenic CO_2 concentrations decrease away from the outcrop. On this deeper surface, however, slower ventilation results in stronger gradients and large areas where the anthropogenic CO_2 is below detection level. The Atlantic contains substantially higher anthropogenic CO_2 concentrations on the 27.3 σ_θ surface than the other basins, due in part to faster ventilation, but also because of the more favorable Revelle Factor. Although the formation of intermediate, mode and deep waters provides the primary mechanism for moving anthropogenic CO_2 into the ocean interior, the magnitude and

distribution of the anthropogenic signal can be quite different depending on the nature of the water mass. As examples, some of the dominant intermediate water masses are outlined in Fig. 2 (*14*).

Antarctic Intermediate Water (AAIW) is formed in the Southern Ocean from upwelled Circumpolar Deep Water in the vicinity of the Subantarctic Front between 45° and 55°S and is then subducted and transported northward at intermediate depths. Immediately north of the AAIW, sub-Antarctic Mode water (SAMW) forms north of the sub-Antarctic Front and contains a greater component of subtropical water than AAIW and is also subducted into the main thermocline of the ocean interior. While at the surface, these water masses appear to take up large amounts of anthropogenic CO_2 from the atmosphere as a result of both high wind speeds enhancing gas transfer and low initial anthropogenic CO_2 content. These subducted intermediate and mode waters contain high concentrations of anthropogenic CO_2, which are transported equatorward and downward, as clearly evidenced by the deepening of anthropogenic CO_2 penetration in Fig. 2. This transport plus the large volumetric contribution of the water masses to the Southern Hemisphere thermocline leads to high anthropogenic CO_2 inventories, estimated to be over 20 Pg C (*14*).

About 3.2 Pg of anthropogenic carbon is found in the North Pacific Intermediate Water (NPIW). Unlike the AAIW that typically delineate the lower limit of the anthropogenic penetration, a substantial amount of anthropogenic CO_2 can be found deeper than the NPIW at the latitude of the section shown in Fig. 2b. NPIW is not the only intermediate type water mass formed in the North Pacific and the complex interplay

of different intermediate type waters in the North Pacific make it difficult to attribute the anthropogenic signal to any one specific intermediate water mass in this region.

Nearly 3 Pg C can be found in the intermediate waters of the northern Indian Ocean (Fig. 2c). The Indian Ocean is different from the other oceans because of its land locked northern boundary. Anthropogenic CO_2 in the tropical north Indian Ocean generally penetrates deeper than in the tropical Atlantic and Pacific. This primarily reflects the introduction of relatively young, dense waters that are high in anthropogenic CO_2 from the Red Sea and the Persian Gulf (*8, 15-16*). Excess evaporation in these regions increases the salinity and density of the waters, which sink and carry the anthropogenic CO_2 with them. As these waters flow into the northern Indian Ocean at intermediate depths, they mix and spread equatorward across the northern Indian Ocean.

Globally, only 7% of the total anthropogenic CO_2 is found deeper than 1500 m. The only place where significant concentrations of anthropogenic CO_2 penetrate to mid and abyssal depths is the North Atlantic as a result of the formation and downward spreading of Labrador Sea Water and North Atlantic Deep Water (NADW). Moving southward away from the formation region, the concentration of anthropogenic CO_2 in NADW decreases because the older waters were exposed to lower atmospheric CO_2 perturbations, and because of mixing with adjacent bottom waters containing little or no anthropogenic CO_2. In total, nearly 7 Pg of anthropogenic carbon is associated with NADW (*14*). Thus, NADW contains substantially less anthropogenic CO_2 than AAIW, despite the fact that NADW has a tremendous impact on the large-scale circulation of the ocean.

There is little anthropogenic CO_2 associated with Antarctic Bottom Water, although exact reconstructions of the anthropogenic CO_2 concentration in this water mass were hampered because of limited carbon data available in regions where these bottom waters are forming. The low anthropogenic CO_2 inventories in these water masses are thought to result from a very high Revelle Factor (Fig. 3), the limited contact with the surface before being transported into the ocean interior and the physical barriers to CO_2 uptake from the presence of sea-ice (*17*). In addition, the anthropogenic CO_2 signals acquired at the surface are quickly diluted with older waters that contain no anthropogenic CO_2 as they sink into the abyssal ocean.

Because most of the deep ocean waters have not been in contact with the atmosphere during the anthropocene (*18*), the 1994 inventory of anthropogenic CO_2 in the ocean is only ~15% of the inventory it would have if the average surface concentration of anthropogenic CO_2 (56 μmol kg^{-1}) were found throughout the ocean. This scenario, however, does not account for the Revelle Factor which makes the uptake capacity of the deep and intermediate waters much lower than the surface waters. Calculating the DIC increase from an 80 ppm change in global ocean pCO_2 values (equivalent to the 1994 atmospheric CO_2 increase from preindustrial), implies that the 1994 inventory is approximately 30% of the ocean potential at that time.

The ocean's role in the global carbon cycle

The global ocean inventory estimated here permits us, for the first time, to place observational constraints on the anthropogenic CO_2 budget for the anthropocene. In particular, it permits us to estimate the magnitude of the time integrated terrestrial carbon

balance which cannot be easily deduced from observations. We first consider the anthropogenic budget terms that are relatively well constrained. Over the anthropocene, about 244±20 Pg C was emitted into the atmosphere as a result of the burning of fossil fuels and cement production (*19*) (Table 1). About two thirds of these emissions have remained in the atmosphere, increasing the atmospheric CO_2 concentration from about 281±2 ppm in 1800 (*20*) to 359±0.4 ppm in 1994 (*21*) translating to an increase of 165 Pg C. Subtracting our ocean inventory estimate of 118±19 Pg C and the atmospheric inventory change from the integrated fossil fuel emissions constrains the net carbon balance of the terrestrial biosphere to be a net source of 39±28 Pg C for the period between 1800 and 1994.Therefore the ocean has constituted the only true net sink for anthropogenic CO_2 over the last 200 years. Without this oceanic uptake, atmospheric CO_2 would be about 55 ppm higher today than what is currently observed (~370 ppm).

The terrestrial net source represents a balance between CO_2 emissions from land-use change, and an uptake of CO_2 by the terrestrial biosphere. Emissions from land-use change are ill constrained. By comparing carbon storage between potential natural vegetation and present-day land cover, deFries *et al.* (*22*) estimated a total loss of about 180 to 200 Pg C since the mid holocene. Using a carbon accounting model for land-use change, Houghton and Hackler (*2*) estimated a carbon loss of about 143 Pg C for the period from 1850 to 1994, with an uncertainty of about 50%. Extrapolating their estimate back to 1800 gives a loss of about 160 Pg C for the anthropocene. Comparisons of land-use change emissions between different estimates for the last two decades reveal, however, that Houghton and Hackler's estimates tend to be nearly twice as large as others

(*23*). Taking this factor into account and the large uncertainty associated with these estimates, we adopt a range of 100 to 180 Pg C for land-use change emissions between 1800 and 1994. With this range, we infer that the terrestrial biosphere must have taken up between 61 and 141 Pg C from the atmosphere over the anthropocene.

It is interesting to contrast this anthropogenic CO_2 budget over the anthropocene with that over the last two decades (*23*). Note that the emissions from fossil fuel and cement production in the decades of the 1980s and 1990s are nearly half of the anthropocene emissions (Table 1). The airborne fraction, i.e. the fraction of the combined fossil fuel and land use emissions that remains in the atmosphere is statistically indistinguishable between the two periods, i.e. 39-48% for the anthropocene versus ~46% for 1980 to 1999 (Table 1). There is an indication, although not statistically significant, that the ocean uptake fraction has decreased from 28-34% to about 26%, while the sink strength of the terrestrial biosphere appears to have remained constant within the large uncertainty bounds (18-33% versus 28%).

Future changes

On the time scales of several thousands of years, it is estimated that ~90% of the anthropogenic CO_2 emissions will end up in the ocean (*24*). Because of the slow mixing time of the ocean, however, the current oceanic uptake fraction is only about one third of this value. Studies of the coupled carbon-climate system have suggested that on decadal time scales the ocean may become a less efficient sink for anthropogenic CO_2 because of positive feedbacks in the coupled carbon-climate system (*25*); consistent with the suggestion of a decreasing ocean uptake fraction noted from Table 1.

There is a potential for both positive and negative feedbacks between the ocean and atmosphere, including changes in both the physics (e.g. circulation, stratification) and biology (e.g. export production, calcification) of the ocean. These processes are still not well understood. On the time scales of decades to centuries, however, most of the known chemical feedbacks are positive. If the surface ocean pCO_2 concentrations continue to increase in proportion with the atmospheric CO_2 increase, a doubling of atmospheric CO_2 from pre-industrial levels will result in a 30% decrease in carbonate ion concentration and a 60% increase in hydrogen ion concentration. As the carbonate ion concentration decreases, the Revelle Factor increases and the ocean's ability to absorb more CO_2 from the atmosphere is diminished. The impact of this acidification can already be observed today and can have ramifications for the biological feedbacks in the future (*26*). If indeed the net feedbacks are primarily positive, the required socio-economic strategies to stabilize CO_2 in the future will be much more stringent than in the absence of such feedbacks. Future studies of the carbon system in the oceans should be designed to identify and quantitatively assess these feedback mechanisms to provide input to models that will determine the ocean's future role as a sink for anthropogenic CO_2.

References and Notes

1. P. J. Crutzen, E. F. Stoermer. *Global Change Newsletter* **41**, 12 (2000).

2. R. A. Houghton, J.L. Hackler, in *Trends: A Compendium of Data on Global Change* (CDIAC, Oak Ridge, TN, 2002).

3. C. Prentice *et al.*, in *Climate Change 2001: The scientific basis. Contribution of working group I to the Third Assessment Report of the Intergovernmental Panel on*

Climate Change., J.T. Houghton *et al.*, Eds. (Cambridge Univ. Press, New York, 2001), pp. 183-237.

4. D. W. R. Wallace, in *Ocean Circulation and Climate*, G. Siedler, J. Church, W. J. Gould, Eds. (Academic Press, San Diego, CA, 2001) pp. 489-521.
5. R. M. Key *et al.*, *Global Biogeochem. Cycles*, in revision, (2004).
6. Bottle data and one degree gridded distributions are available through GLODAP web site <http://cdiac.esd.ornl.gov/oceans/glodap/Glodap_home.htm>
7. N. Gruber, J. L. Sarmiento, T. F. Stocker, *Global Biogeochem. Cycles* **10**, 809 (1996).
8. C. L. Sabine *et al.*, *Global Biogeochem. Cycles* **13**, 179 (1999).
9. C. L. Sabine *et al.*, *Global Biogeochem. Cycles* **16**, 1083, doi: 10.1029/2001GB001639 (2002).
10. K. Lee *et al.*, *Global Biogeochem. Cycles* **17**, 1116, doi: 10.1029/2003GB002067 (2003).
11. Materials and methods are available as supporting material on *Science* Online.
12. R. Revelle, H.,E. Suess, *Tellus* **9**, 18 (1957).
13. T. Takahashi, J. Olafsson, J. G. Goddard, D. W. Chipman, S. C. Sutherland, *Global Biogeochem. Cycles* **7**, 843 (1993).
14. Five intermediate water masses and North Atlantic Deep Water (NADW) were defined using the following temperature (T) and salinity (S) properties: Pacific AAIW: 33.8<S<34.5 and 2<T<10; NPIW: S<34.3 and 5<T<12; Indian AAIW: 33.8<S<34.5 and 2<T<10; Red Sea Water: S>34.8 and 5<T<14; Atlantic AAIW: 33.8<S<34.8 and 2<T<6; NADW: 34.8<S<35 and 1.5<T<4. Water mass inventories

were determined by summing up the gridded anthropogenic CO_2 values within a region defined by the T and S limits using the Levitus World Ocean Atlas 2001 salinity and temperature fields.

15. A. Papaud, A. Poisson, *J. Mar. Res.* **44**, 385 (1986).
16. S. Mecking, M. Warner, *J. Geophys. Res.* **104**, 11087 (1999).
17. A. Poisson, C.-T. A. Chen, *Deep Sea Res*. Part A **34**, 1255 (1987).
18. M. Stuiver, P. D. Quay, H. G. Ostlund, *Science* **219**, 849 (1983).
19. G. Marland, T. A. Boden, R. J. Andres, in *Trends: A Compendium of Data on Global Change* (CDIAC, Oak Ridge, TN, 2004).
20. D. M. Etheridge *et al.*, *J. Geophys. Res.* **101**, 4115 (1996).
21. C. D. Keeling, T. P. Whorf, in *Trends: A Compendium of Data on Global Change* (CDIAC, Oak Ridge, TN, 2004).
22. R. S. de Fries, C. B. Field, I. Fung, G. J. Collatz, L. Bounoua, *Global Biogeochem. Cycles* **13**, 803 (1999).
23. C. L. Sabine *et al.*, in *The Global Carbon Cycle: Integrating Humans, Climate, And The Natural World. SCOPE 62*, C. B. Field, M. R. Raupach, Eds. (Island Press, Washington D.C., 2004) pp. 17-44.
24. D. E. Archer, H. Kheshgi, E. Maier-Reimer, *Global Biogeochem. Cycles* **12**, 259 (1998).
25. N. Gruber *et al.*, in *The Global Carbon Cycle: Integrating Humans, Climate, And The Natural World. SCOPE 62*, C. B. Field, M. R. Raupach, Eds. (Island Press, Washington D.C., 2004) pp. 45-76.

26. R. A. Feely *et al.*, *Science*, in revision (2004).

27. We thank all of those that contributed to the global data set complied for this project, including those responsible for the hydrographic, nutrient, oxygen, carbon, CFC measurements, and the Chief Scientists. The amount of work that went into collecting, finalizing, and synthesizing these data in a manner that makes a publication like this possible, can never be properly acknowledged. This work was funded by grants from NOAA/DOE and NSF. Partial support for KL also provided by the AEBRC at POSTECH. PMEL contribution number 2683.

Supporting Online Material

www.sciencemag.org

Materials and Methods

Fig. S1

Table S1

Figure 1. Column inventory of anthropogenic CO_2 in the ocean (mol m^{-2}). High inventories are associated with Deep Water formation in the North Atlantic and Intermediate and Mode Water formation between 30°-50°S. Total inventory of shaded regions is 106±17 Pg C.

Figure 2. Representative sections of anthropogenic CO_2 (μmol kg^{-1}) from the Atlantic (A), Pacific (B) and Indian (C) oceans. Grey hatched regions and numbers indicate distribution of intermediate water masses (and North Atlantic Deep Water) on the given section and the total inventory of anthropogenic CO_2 (Pg C) within these water masses. The southern water masses in each ocean represent Antarctic Intermediate Water. The northern water masses represent the North Atlantic Deep water, North Pacific Intermediate Water, and Red Sea/Persian Gulf Intermediate water in panels a, b, and c, respectively. The two heavy lines on each section give the potential density contours for the surfaces shown in figure 4. Inserts show maps of the cruise tracks used. Note that the depth scale for (A) is twice that of the other figures reflecting the deeper penetration in the North Atlantic.

Figure 3. Map of the 1994 distribution of Revelle Factor, $(\delta pCO_2/\delta DIC)/(pCO_2/DIC)$, averaged for the upper 50 m of the watercolumn. High Revelle Factor indicates that, for a given atmospheric CO_2 perturbation, the oceanic equilibrium concentration of anthropogenic CO_2 will be lower than low Revelle Factor waters. The current Revelle Factors are about one unit higher than they were in the preindustrial ocean.

Figure 4. Maps of anthropogenic CO_2 on the 26.0 (A) and 27.3 (B) potential density surfaces. Heavy lines at the edge of colored region indicate areas where the density

surface outcrops. The highest values are generally observed closest to the outcrop and decreasing toward the equator.

Table 1: Anthropogenic CO_2 budget for the anthropocene (1800-1994) and for the decades of the 1980s and 1990s.

CO_2 Sources	1800-1994 [Pg C]*		1980-1999 [Pg C]¶
Constrained sources and sinks			
(1) Emissions from fossil fuel and cement production	244†	± 20	117±5
(2) Storage in the atmosphere	-165‡	± 4	-65±1
(3) Uptake and storage in the ocean	-118§	± 19	-37±8
Inferred net terrestrial balance			
(4) Net terrestrial balance = [-(1)-(2)-(3)]	39	± 28	-15±9
Terrestrial balance			
(5) Emissions from land use change	100 to 180‖		24±12
(6) Terrestrial biosphere sink = [-(1)-(2)-(3)]-(5)	-61 to -141		-39±18

* Errors as estimated by respective sources; errors of sums and differences are calculated by quadratic error propagation.

†From (*19*), with an error estimate of ±8%

‡Calculated from change in atmospheric pCO_2 (1800: 281±2 ppm; 1994: 359±0.4 ppm)

§This study, includes anthropogenic CO_2 storage in marginal seas and Arctic Ocean.

‖Based on (*2*), see text for details.

¶From (*23*), integrated for the 1980 to 1999 period.

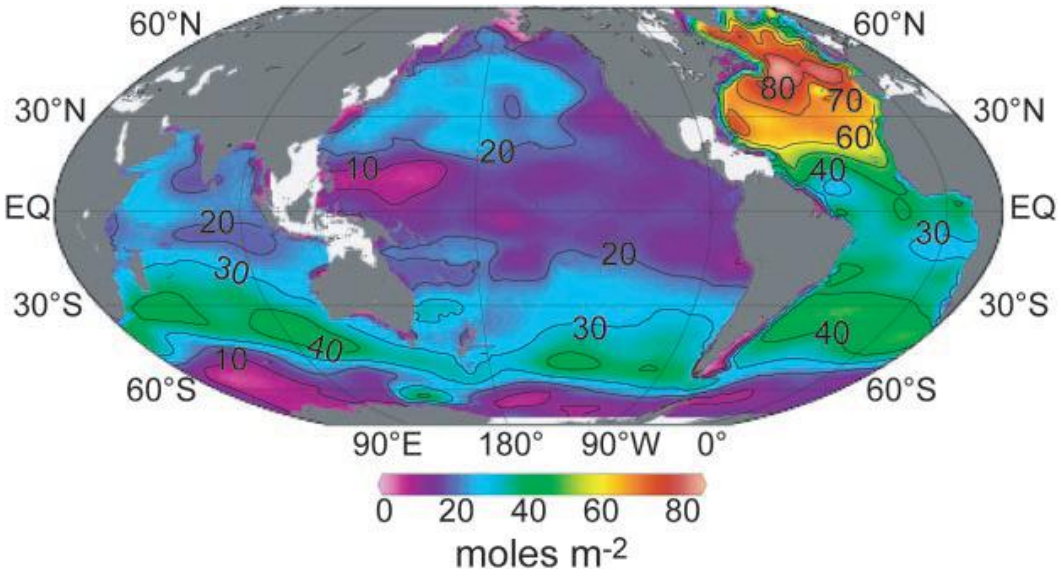
60°N
60°N
30°N
30°N
EQ
EQ
30°S
30°S
60°S
60°S
90°E
180°
90°W
0°
0
20
40
60
80
moles m-2
80
70
60
40
30
20
10
0
20
30
40
10
20
30
40

Fig. 1.

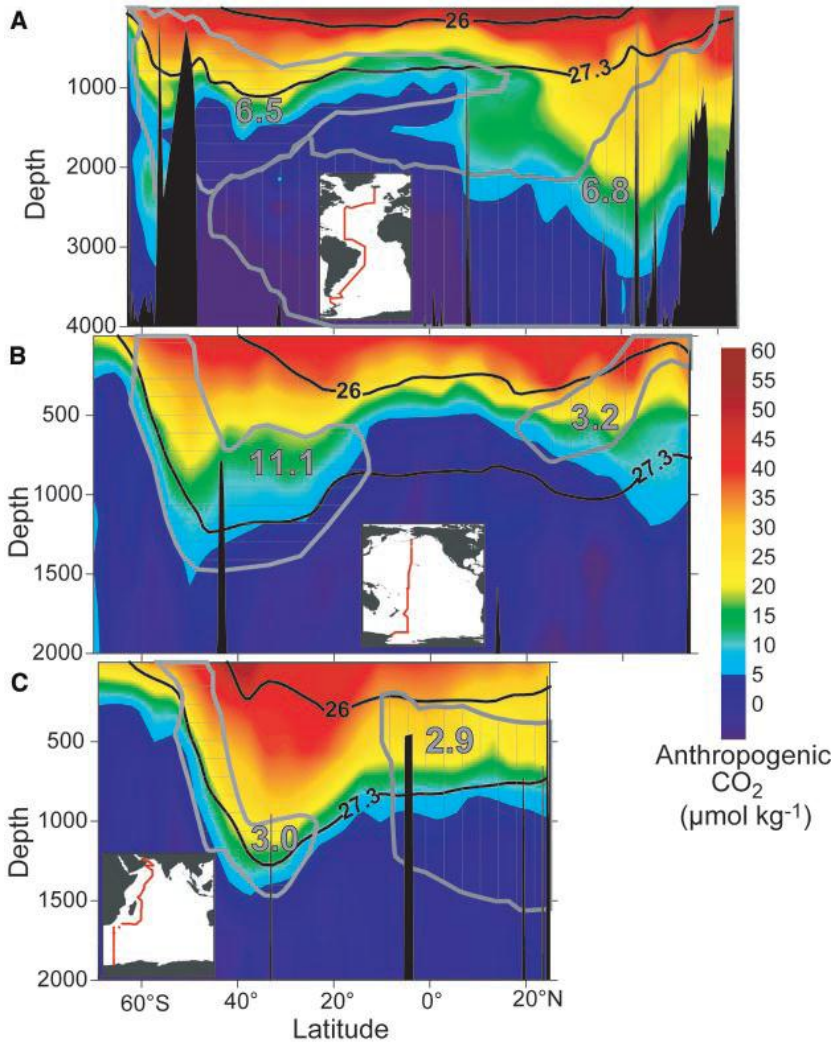
A
B
C
Depth
1000
2000
3000
4000
500
1500
26
27.3
6.5
6.8
11.1
3.2
2.9
3.0
60
55
50
45
40
35
30
25
20
15
10
5
0
Anthropogenic
CO2
(µmol kg-1)
60°S
40°
20°
0°
20°N
Latitude

Fig. 2.

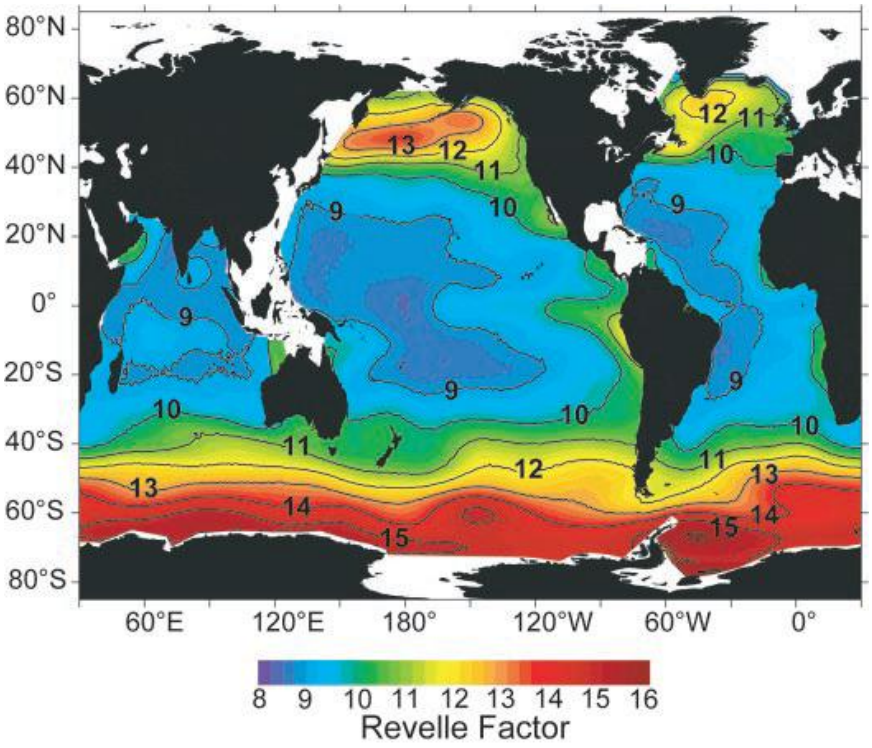
80°N
60°N
40°N
20°N
0°
20°S
40°S
60°S
80°S
60°E
120°E
180°
120°W
60°W
0°
8 9 10 11 12 13 14 15 16
Revelle Factor

Fig. 3

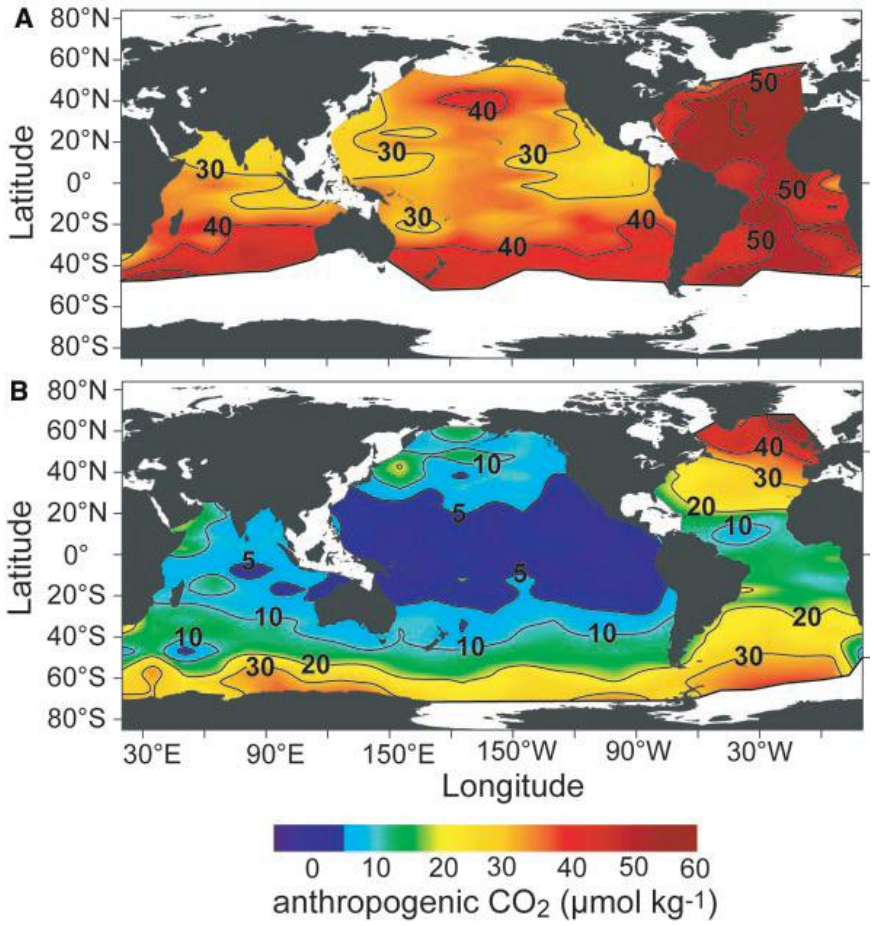
A
B
80°N
60°N
40°N
20°N
0°
20°S
40°S
60°S
80°S
Latitude
30°E
90°E
150°E
150°W
90°W
30°W
Longitude
0 10 20 30 40 50 60
anthropogenic CO2 (µmol kg-1)

Fig. 4.

Science Supporting Online Material

The oceanic sink for anthropogenic CO_2

Christopher L. Sabine, Richard A. Feely, Nicolas Gruber, Robert M. Key, Kitack Lee, John L. Bullister, Rik Wanninkhof, C.S. Wong, Douglas W.R. Wallace, Bronte Tilbrook, Frank J. Millero, Tsung-Hung Peng, Alexander Kozyr, Tsueno Ono, and Aida F. Rios

Methods and Materials

Brewer (*S1*) and Chen and Millero (*S2*) made the first attempts to separate the relatively small anthropogenic CO_2 signal from measured DIC values nearly 25 years ago. They assumed that anthropogenic CO_2 could be estimated by correcting measured sub-surface DIC concentrations for the contributions of organic matter decomposition and dissolution of carbonate minerals and taking into account the DIC concentration the water had in the preindustrial ocean when it was last in contact with the atmosphere, referred to as preformed DIC. Since the preindustrial ocean DIC concentrations were not measured, the large preformed DIC component was estimated from empirical relationships with nutrients and temperature and an assumption that the deep ocean contains no anthropogenic CO_2. Gruber *et al.* (*S3*) improved the separation method by defining a quasi-conservative tracer, C*, that separates the preformed DIC into an equilibrium component that can be calculated from thermodynamics, and a substantially smaller disequilibrium component. Another strength of this approach is that it is not as strongly affected by mixing as the former methods. The separation can be summarized by:

$$DIC^{(anth)}\ (\mu mol\ kg^{-1}) = DIC^{(meas)} - \Delta DIC^{(bio)} - DIC^{(eq)} - \Delta DIC^{(diseq)} \qquad (1)$$

Where $DIC^{(anth)}$ is the anthropogenic CO_2 concentration of a sub-surface water sample; $DIC^{(meas)}$ is the measured DIC concentration; $\Delta DIC^{(bio)}$ is the change in DIC as a result of

biological activity (both organic carbon and $CaCO_3$ cycling); $DIC^{(eq)}$ is the DIC of seawater (at the temperature, salinity, and preformed alkalinity of the sample) in equilibrium with a pre-industrial CO_2 partial pressure of 280 μatm; and $\Delta DIC^{(diseq)}$ is the air-sea CO_2 disequilibrium a water parcel had when it was last in contact with the atmosphere, expressed in μmol kg^{-1} of DIC.

The first three terms on the right side of the equation can be calculated explicitly for each water sample and are called ΔC*:

$$\Delta C^* = DIC^{(meas)} - DIC^{(eq)} + 117/170(O_2 - O_2^{(sat)}) - 1/2(TA - Alk0 - 16/170(O_2 - O_2^{(sat)})) + 106/104 N^*_{anom} \quad (2)$$

where $DIC^{(meas)}$, TA and O_2 are the measured concentrations for a given water sample in μmol kg^{-1}; $Alk0$ is the preformed alkalinity value; $O_2^{(sat)}$ is the calculated oxygen saturation value that the waters would have if they were adiabatically raised to the surface; and N^*_{anom} is the net denitrification signal in the waters. $Alk0$ was estimated for each basin using a multiple linear regression of the surface alkalinity values to conservative tracers.

For any given water parcel in the interior of the ocean, the net air-sea disequilibrium value represents the weighted average of individual air-sea disequilibria from various source waters. We adopted an optimum multiparameter (OMP) analysis to evaluate the relative contributions of the different water sources on individual isopycnal surfaces. Two methods were then used to estimate the disequilibrium correction, $\Delta DIC^{(diseq)}$, for the different water sources (Eq. 1). For shallow or ventilated isopycnal surfaces that contain measurable levels of chlorofluorocarbons (CFC), the $\Delta DIC^{(diseq)}$ terms for the water sources were derived from the CFC-12 corrected ΔC* calculation,

ΔC^*_{t12}. ΔC^*_{t12} is derived in the same manner as ΔC^*, but rather than evaluating the carbon concentration the waters would have in equilibrium with a preindustrial atmosphere, they were evaluated with respect to the CO_2 concentration the atmosphere had when the waters were last at the surface based on the concentration ages determined from CFC-12 measurements. For isopycnal surfaces located in the interior of the ocean where CFC-12 is absent and where one can reasonably assume that there is no anthropogenic CO_2, the ΔC^* values in these waters are equal to $\Delta DIC^{(diseq)}$. To ensure that the $\Delta DIC^{(diseq)}$ values for deep density surfaces were not contaminated with anthropogenic CO_2, we only used ΔC^* values showing no obvious trend along the isopycnal surface.

To generate a global anthropogenic CO_2 inventory, the individual sample estimates from the Indian (*S4*), Pacific (*S5*), and Atlantic (*S6*) oceans were objectively gridded (*S7*) onto 33 depth surfaces with one degree resolution. These three sets of maps where merged with a fourth set of maps that was separately generated for the Southern Ocean. An error weighted mean was calculated for grid cells with more than one estimated value. Since the global survey had limited data coverage in the marginal basins (the South China Sea/Indonesian region, Yellow Sea, Japan/East Sea, Sea of Okhotsk, Gulf of Mexico, North Sea, Mediterranean Sea, and the Red Sea) and the Arctic Ocean (north of 65°N), these areas were excluded from the mapped regions.

The uncertainty in the total inventory is estimated to be approximately 16% based on uncertainties in the anthropogenic CO_2 estimates and mapping errors. Uncertainties in the former arise from both random errors and potential biases. The random errors, including the precision of the original measurements, have been estimated to be about ±8

μmol kg^{-1} (*S3-6, S8*). This estimate is about twice as large as the standard deviation of the ΔC* values below the deepest anthropogenic CO_2 penetration depth suggesting that the propagated errors may be a maximum estimate of the random variability. Based on these estimates, the limit of detection for this technique is assumed to be approximately 5 μmol kg^{-1}. The impact of these random errors on the uncertainty of the inventory is negligible, as a large number of samples were averaged to estimate the inventory.

The potential biases in the technique are much more difficult to evaluate and could include errors in the 1) biological correction resulting from the assumed stoichiometric relationships, 2) water mass age estimates based on CFCs, 3) assumption of minimal diapycnal mixing, 4) assumption that oxygen was in equilibrium in surface waters and 5) that the air-sea disequilibrium term is constant over time. Biases in the technique have been primarily evaluated with sensitivity studies and comparisons with other approaches (e.g. *S3-6, S8-12*). These studies estimated the potential biases to be about 10-15%. The mapping errors can be estimated from the objective mapping calculations (*S7*), but are also difficult to assess quantitatively since the mapping errors are highly correlated both vertically and horizontally (*S13*). We assume that their contribution is smaller than 15%.

To arrive at a full global ocean inventory, we assume that the inventory in the unmapped regions south of 65°N (the marginal basins) scales with ocean surface area. This adds about 6 Pg C to the total. Including the Arctic Ocean (defined here as all ocean north of 65°N) using an area scaling approach would increase the total by about 3-4% to 116.5 Pg C. Willey *et al.* (*S14*) found that the Arctic Ocean accounted for approximately 5% of the global ocean CFC inventory in 1994. Given the correlation between CFC and

anthropogenic CO_2 inventories (*S15*), we adopt the scaling based on CFC inventories for the Arctic Ocean, and arrive at our final global anthropogenic CO_2 inventory estimate of 118±19 Pg C. This inventory pertains to a nominal year of 1994, approximately the median year of our oceanographic measurements.

References

S1. P. G. Brewer, *Geophys. Res. Lett.* **5**, 997 (1978).

S2. C.-T. A. Chen, F. J. Millero, *Nature* **277**, 205 (1979).

S3. N. Gruber, J. L. Sarmiento, T. F. Stocker, *Global Biogeochem. Cycles* **10**, 809 (1996).

S4. C. L. Sabine *et al.*, *Global Biogeochem. Cycles* **13**, 179 (1999).

S5. C. L. Sabine *et al.*, *Global Biogeochem. Cycles* **16**, 1083, doi: 10.1029/2001GB001639 (2002).

S6. K. Lee *et al.*, *Global Biogeochem. Cycles* **17**, 1116, doi:10.1029/2003GB002067 (2003).

S7. J. L. Sarmiento, J. Willebrand, S. Hellerman, *Objective analysis of Tritium observations in the Atlantic Ocean during 1971-74, OTL Tech Rept. #1*, (Princeton University, Princeton, NJ, 1982).

S8. N. Gruber, *Global Biogeochem. Cycles* **12**, 165 (1998).

S9. R. Wanninkhof *et al.*, *Tellus* **51B**, 511, 1999.

S10. C. Coatanoan, C. Goyet, N. Gruber, C. L. Sabine, M. Warner, *Global Biogeochem. Cycles* **15**, 11 (2001).

S11. C. L. Sabine, R. A. Feely, *Global Biogeochem. Cycles* **15**, 31 (2001).

S12. F. F. Pérez, M. Álvarez, A. F. Ríos, *Deep-Sea Res. I* **49**, 859 (2002).

S13. R. M. Key *et al.*, *Global Biogeochem. Cycles,* in revision (2004).

S14. D. A. Willey *et al.*, *Geophys. Res. Lett.* **31**, L01303, doi:10.1029/2003GL018816 (2004).

S15. B. I. McNeil, R. J. Matear, R. M. Key, J. M. Bullister, J. L. Sarmiento, *Science* **299**, 235 (2003).

Figure S1. Zonal total inventory (A) determined by vertically integrating the anthropogenic CO_2 in each one degree grid then summing up for each degree of latitude, and zonal mean inventory (B) determined by taking the vertically integrated values and dividing by the area of each grid box and averaging for each degree of latitude. Zonal mean inventory shows that the Atlantic generally has the highest average inventories on a per square meter basis, but when the total area is taken into consideration, the Pacific has the highest total inventories everywhere except north of 20°N.

Table S1. Distribution of Anthropogenic CO_2 inventories in Pg C by basin and latitude band for 1994.

	Atlantic	Pacific	Indian	World
50-65°N	4	1	-	5 (5%)
14-50°N	16	11	1	28 (26%)
14°S-14°N	7	8	6	21 (20%)
14-50°S	11	18	13	42 (40%)
>50°S	2	6	2	10 (9%)
total	40 (38%)	44 (41%)	22 (21%)	106

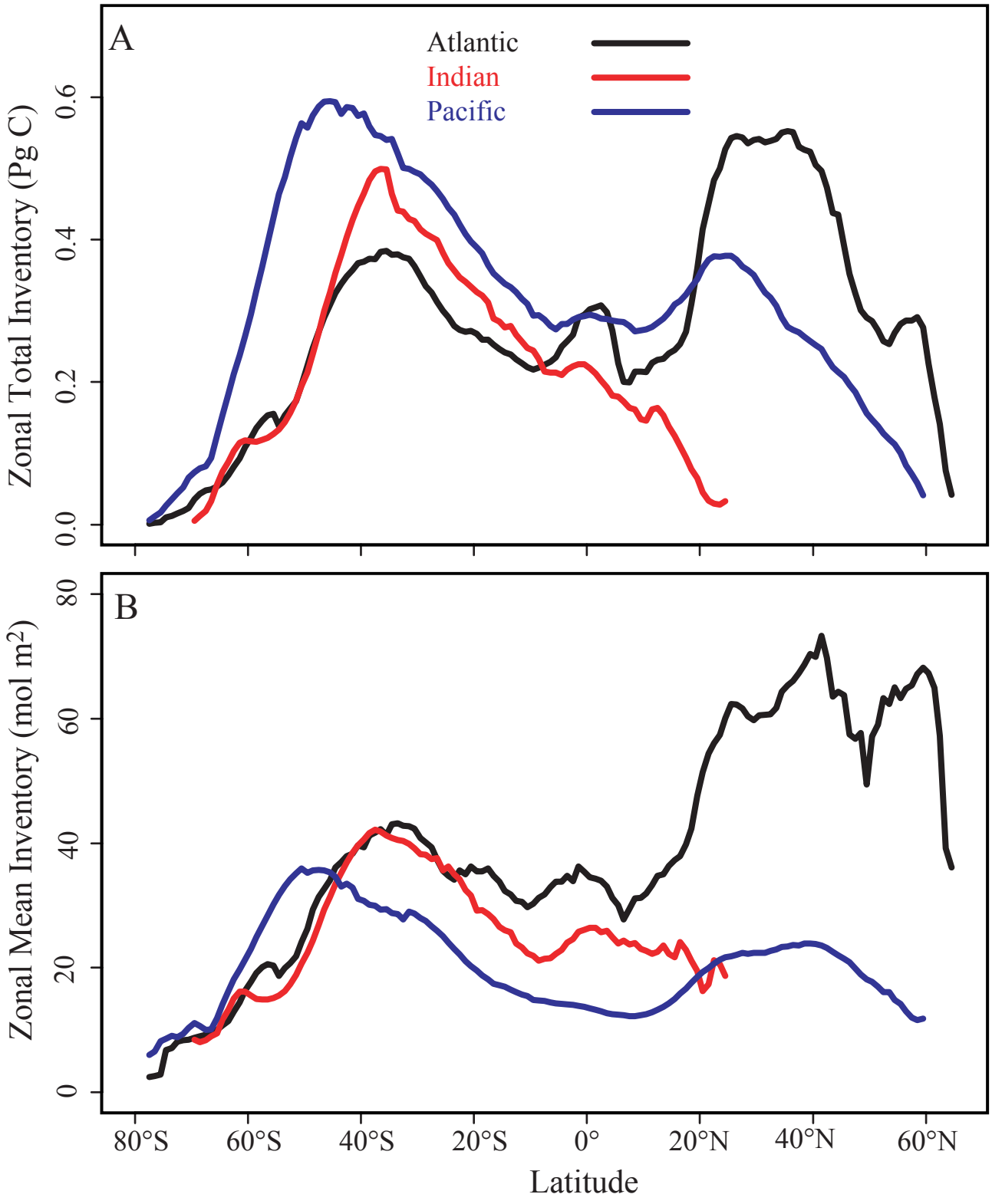
A
Atlantic
Indian
Pacific
Zonal Total Inventory (Pg C)
0.0
0.2
0.4
0.6
B
Zonal Mean Inventory (mol m2)
0
20
40
60
80
80°S
60°S
40°S
20°S
0°
20°N
40°N
60°N
Latitude